

# BUCKLING STRENGTH ANALYSES OF CORRODED TRUSS MEMBER WITH COMBINED CROSS SECTION

SAE TERANISHI<sup>1</sup>, TATSUMASA KAITA<sup>1</sup>, TATSURO YAMANE<sup>2</sup>, SHUHEI KAWAMI<sup>3</sup>,  
and KATASHI FUJII<sup>4</sup>

<sup>1</sup>*Dept of Civil Engineering and Architecture, Tokuyama College of Technology, Shunan,  
Japan*

<sup>2</sup>*Graduate School of Science and Engineering, Ehime University, Matsuyama, Japan*

<sup>3</sup>*Chuden Engineering Consultants Corporation, Hiroshima, Japan*

<sup>4</sup>*Graduate School of Engineering, Hiroshima University, Higashi-Hiroshima, Japan*

It will be important to forecast future the deterioration of remaining strength on corroded members for working out reasonable maintenance scenarios on steel structure. In this study, the buckling strength analyses, including future forecast, were conducted for the vertical member, which has the combined cross-section in actual aging truss bridge. For constructing the analytical model, a simple corrosion progress model was applied to generating the corroded steel surface. In this corrosion progress model, it assumes that corrosion pits are generated by the attack factors which can be decided by some control parameters for corrosion environment, corrosion form and corrosion area. And, the constant number of the attack factors per year fall all over the discretized steel surface. The corrosion surface in the future can be generated numerically by repeating mentioned above. The average thickness calculated from the numerical corrosion surface was applied to the local corrosion area in each analytical model. From these analytical results, a future forecast method applying a corrosion progress model was discussed by focusing on the aging deterioration of the buckling strength.

*Keywords:* Local corrosion, Corrosion progress model, Elastic buckling, Pitting corrosion, Remaining thickness, Finite element analysis.

## 1 INTRODUCTION

Though corrosion damages of the aging steel bridge will often progress locally at the member, which has complicated structural details, it is not easy to remove corrosion cause and to prevent re-deterioration of painting. Therefore, it will be important to predict future deterioration of the remaining strength on corroded members for drawing reasonable maintenance scenarios on the steel bridge. Also, if current corrosion damages make further progress, it will be thought the collapse behavior of compressive members and the whole bridge also may be changed for the worse. However, even if the remaining strength has deteriorated slightly, it will be the fact that it may not be much problem from the viewpoint of required performance and actual usability in a local bridge with comparatively a low-traffic condition.

In this study, the buckling strength analyses using FEM, including future forecast, were conducted for the vertical member, which has the combined section in the actual aging truss bridge. A simple corrosion progress model (Fujii *et al.* 2010) was applied to generating the

corroded steel surface of this analytical model. In this corrosion progress model, it assumes that corrosion pits are generated numerically by the attack factors, which can be decided by some control parameters for corrosion environment, corrosion form and corrosion area. Through this study, one of the examples of future forecast method of remaining strength applying the corrosion progress model to FEM modeling is indicated for more reasonable maintenance planning.

## 2 OUTLINE FOR ANALYZED TRUSS MEMBER

Analyzed vertical member in this study is a part of the main span structure in aging Pratt truss bridge (Figure 1), which had been used for 99 years in Japan. Though this bridge has 2 main spans with a length of 50.19m, the main span of the side of the left bank was focused on this study from the considering with a severer corroded state. All structural members of this truss are the combination member constructed by riveting channel steels and many racing bars, as shown in Figure 2. These corrosion damages were found at the time of periodic inspection in 2012. After that, the repair work using additional plates were carried out immediately for ensuring safety; the field investigation was carried out in 2016 for checking re-degradation of painting and corrosion progress (Yamane *et al.* 2019).

Figure 3 shows the distribution diagram of all severe corrosion damages found by 2 times of field inspection. Both red and blue dots indicate severe damages with a corrosion hole. From this figure, it was clear that the corrosion was progressing certainly at local regions, and these corrosion damages were concentrated to 2 vertical members. On the other hand, the structural detail of joint parts, as shown in Figure 2 becomes like a pocket-form because the sway bracing is inserted to among flanges of the channel steel in vertical members. Therefore, the flowing rainwater along the surface of the sway bracing collects in this pocket with rusts and bird wastes, and a wet state continues for a long time. Also, it will be difficult to remove their rusts and wastes perfectly in this pocket before repainting. In this buckling analysis, the vertical member V9 was assumed as an analytical object because the severest damage with a maximum rate of cross-section loss of 16.4% occurred in this member.

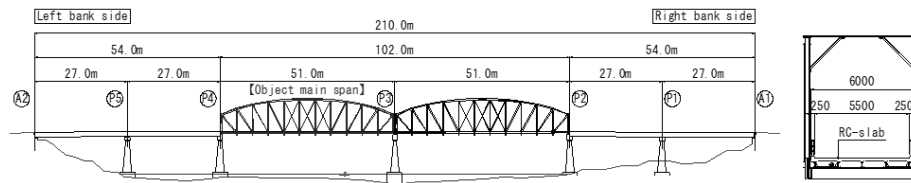


Figure 1. A view of truss used in this study.

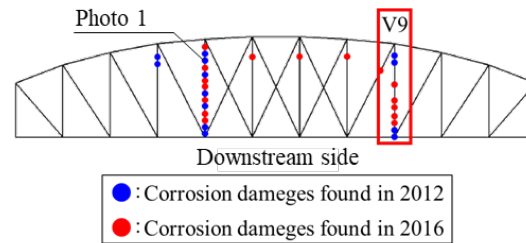
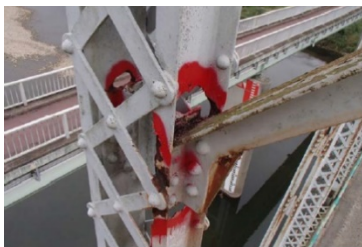


Figure 2. An example of corrosion damage. Figure 3. Distribution diagram of severe corrosion damages.

### 3 BUCKLING STRENGTH ANALYSIS

#### 3.1 Analytical Model and Analytical Conditions

As shown in Figure 4, the analytical models assuming the vertical member V9 were constructed by the shell element with 4 nodes, and all rivet joints were modeled as the rigid connection. The size of each shell element was set to under 30mm square in order to consider the corrosion damages which have a certain area. In the corrosion damage modeling, the maximum corrosion depth was applied to the entire corrosion area based on the results of field inspection.

The material properties of the steel were assumed to be elastic modulus  $E=210$  [GPa], yield stress  $\sigma_y=245$  [MPa], and Poisson's ratio  $\nu=0.3$ . The stress-strain relation was assumed as the perfect elastoplasticity. Boundary conditions of the vertical member were set to be simple support at both ends. Also, the racing bars which connect two-channel steels to each other for keeping the sectional shape were modeled as a continuous plate with a zigzag shape.

#### 3.2 Buckling Strength Analyses for Initial State Model (without Corrosion Damages)

Figure 5 shows a load - deflection curve obtained from the analytical result on the initial state model which has no corrosion damages. The abscissa shows the deflection at center point of effective buckling length. Euler's buckling strength  $P_E$  was calculated by using the cross-section of V9 excepted racing bars. From the consideration of this figure, it can be confirmed that though the racing bars will slightly affect to bending stiffness of member, the difference of buckling strength between  $P_{cr}$  and  $P_E$  was only about 12%. When the thickness of racing bars was reduced to 2mm, the difference also became further small.

Also, the collapse behavior of this model was the elastic buckling about the weak axis as shown in Figure 6.

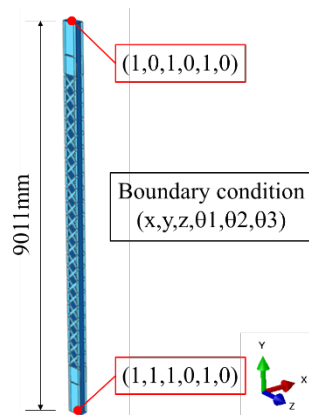


Figure 4. Analytical model.

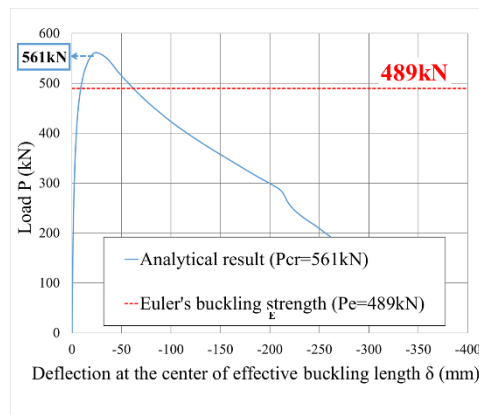


Figure 5. P- $\delta$  relations in initial state.



Figure 6. Buckling deformation.

#### 3.3 Buckling Strength Analyses for Damaged State Model (with Corrosion Damages)

Figure 7 shows the analytical model assuming the actual corrosion damages. The locations of each corrosion damage are compatible with Figure 3. The corrosion hole was expressed by removing in corresponding elements. Other corroded area has a reduced constant thickness by considering the maximum corrosion depth.

Figure 8 shows the load - deflection curves of the damaged state model with that of the initial state model. From the comparison of these curves, it can make sure that though the stiffness was slightly decreased before buckling, the buckling strength  $P_{cr}$  of the damaged model is almost the same as that of the initial state model. It will be mean that the buckling strength of this vertical member will not be almost unaffected by this state of corrosion damages because the buckling strength of V9 will be decided by elastic buckling. Also, it might become one of the reasons that almost corrosion damages were appeared to near both ends of the member.

However, if the remaining thickness in the current corrosion area is more decreased by corrosion, which it is difficult to prevent progress, the influence on buckling strength and collapse behavior of corrosion damages may become large in the future.

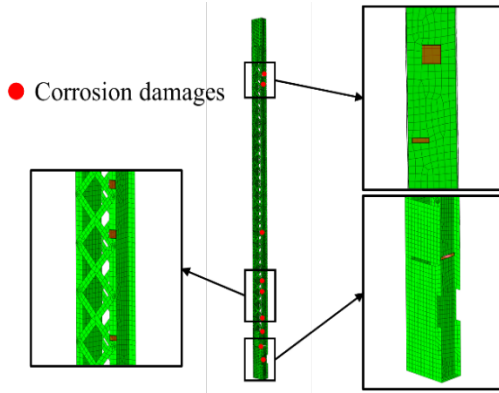


Figure 7. Corrosion damages in analytical.

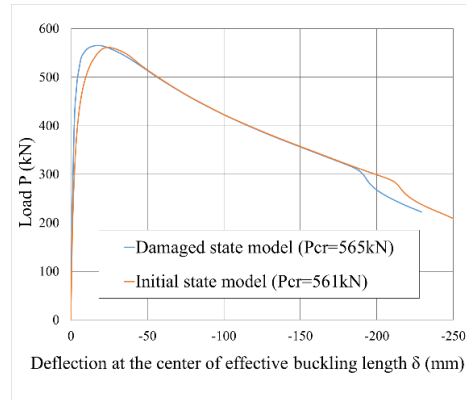


Figure 8. Comparison of P- $\delta$  relations.

## 4 BUCKLING STRENGTH ESTIMATION USING CORROSION PROGRESS MODEL

### 4.1 Outline of Corrosion Progress Model

A corrosion progress model (Fujii *et al.* 2010) which can generate surface irregularities due to corrosion numerically was applied to this analysis for estimating the deterioration of buckling strength in the future. Figure 9 shows the concept image of this corrosion progress model. In nature, though the corrosion will be occurred by oxidation reaction of iron as electrochemical phenomenon, this corrosion progress model supposes that many attack factors fall randomly to the grid points on steel surface discretized to mesh division arbitrarily. This supposition may be similar to generating the ground hole by aerial bombing. One attack factor generates a corrosion hole with the shape following simple Eq. (1).

$$V_i = F \cdot \exp(-\beta d_i) \quad (1)$$

Here,  $V_i$  [mm/year]: corrosion depth of arbitrary grid point,  $F$  [mm/year]: the maximum corrosion depth just below the attack point,  $\beta$ : dumping factor depending on distance and  $d_i$ : distance from the attack point. In this numerical model, the corrosion depth  $V_i$  is calculated by integrating the influence due to multiple attack factors in overlapped affected areas. Also, the shape of surface irregularities in the future can be generated by repeating that the constant number of attack factors  $N$  fall to steel surface every year.

Though it may be difficult to set a suitable value of each parameter for this calculation because corrosion damages have different corrosion environments and corrosion form, it can be

tentatively set by conforming the generating results to the actual remaining thickness obtained from the result of field inspection.

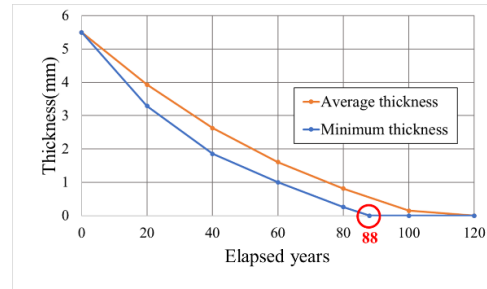
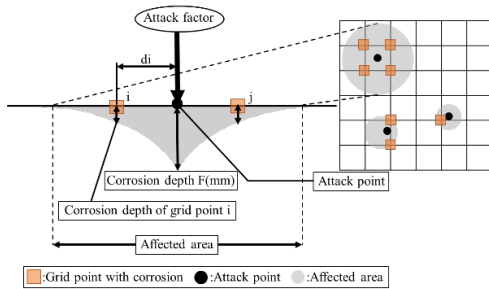


Figure 9. Concept of corrosion progress model. Figure 10. Aging deterioration of remaining thickness.

## 4.2 Buckling Strength Analyses Considered Corrosion Progress

From one of the few maintenance records, since it was able to be assumed that the corrosion holes of V9 had appeared at least 90 years later from construction, each parameter of this corrosion progress model was set to conform to this fact.

Figure 10 shows an example of the aging deterioration of the remaining thickness every 20 years, calculating from generated surface data. It can be confirmed that the minimum thickness was decreased non-linearly with the elapsed year and was reached to zero (corrosion hole) in 88 years later. The size of the corroded region is assumed as 200mm square in this case. Here,  $F=0.3$  [mm/year],  $N=150$  [per year],  $\beta=0.2$ .

The contour maps of the remaining thickness in every 20 years were shown in Figure 11. From these figures, it will be found the corrosion progress behavior and the shape of the steel surface. In this case, the steel surface in the assumed corrosion area was lost perfectly in 120 years later. However, the corrosion-preventing effect of paint did not consider in this simulation because there was nothing left of the painting history.

In this buckling analysis, the average thickness obtained from generated surface data depending on elapsed years were applied to all corrosion area in the analytical model shown in Figure 7, and it was assumed that the corrosion environment was same in all corrosion damages.

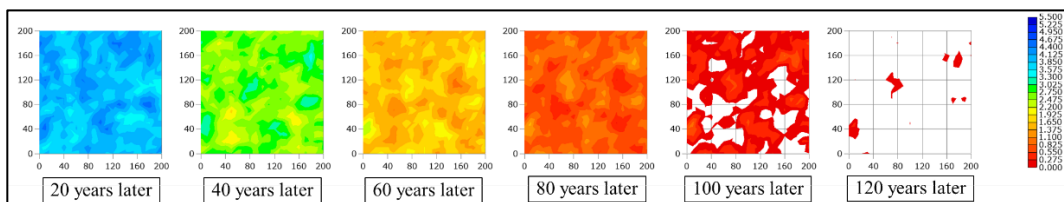


Figure 11. Contour maps of remaining thickness (unit: mm).

## 4.3 Analytical Results and Discussions

Figure 12 shows the aging deterioration of remaining buckling strength from the analytical results of the corrosion progress model. The ordinate axis is the buckling strength ratio ( $P_{cr}/P_{cr0}$ ). From this figure, it should be focused that the buckling strength increases up to 80 years. The reason of this will be thought that the load eccentricities were appeared locally at each corrosion damages

because local sectional loss makes change slightly the position of neutral axis in cross-section. Also, the buckling strength was increased by only 4% for 80 years, and the buckling mode was also almost the same as the initial state as shown in Figure 6, because the buckling strength of this member will be decided by elastic buckling. However, it was confirmed that the buckling strength was decreased from 100 years later. At this time, the buckling mode was clearly changed from global buckling to local buckling near the lower end, which has many corrosion damages.

Though the influence on the buckling and compressive behavior of corrosion progress was small in these analyses, it will be very important to predict the future state analytically for realizing more reasonable bridge maintenance.

On the other hand, the thickness measurement results of corrosion damage for improving the accuracy of the corrosion progress model should be accumulated by utilizing the opportunity of periodic inspection every 5 years in Japan. In doing so, the practical maintenance plan may be able to draw easily with high reliability. Also, it will be required that the parameters should be refined to more suitable settings, which can prepare for various corrosion forms.

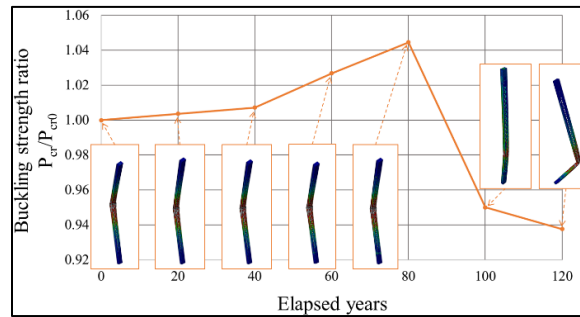


Figure 12. Aging deterioration of remaining buckling strength.

## 5 CONCLUSIONS

In this study, the buckling strength analyses of a corroded truss member with the combined cross-section were carried out, focusing on the elastic buckling. And a simple future forecast method applying the corrosion progress model was proposed from the consideration of aging deterioration of the buckling strength. The main conclusions of this study are as follows:

- 1) Though it may be difficult to set a suitable value of each parameter for the corrosion progress model because corrosion damages have different corrosion environments and corrosion forms, it can tentatively set by conforming the generating results to the actual remaining thickness obtained from the result of field inspection.
- 2) Though the influence on the buckling and compressive behavior of corrosion progress was very small in this study, it will be important to predict aging deterioration analytically using the inspection results for realizing more reasonable bridge maintenance.

## References

- Yamane, T., Kaita, T., Fukuda, H., Kawami, S., Satake, R. Hirahara, Y., Kanou, T., and Fujii, K., *Analytical Study of Ultimate Load Bearing Capacity for an Aging Pratt Truss Bridge using FEM*, Proceedings of Bridge Engineering Institute Conference in 2019 (BEI-2019), Yail, J. K. (eds.), 709-713, 2019.
- Fujii, K., Hashimoto, K., Watanabe, E., Ito, Y., Sugiura, K., Nogami, I., and Nagata, K., *A Prediction Method of Strength Deterioration in Aging of Circular Steel Tube Corroded in Marine Environment* (In Japanese), Journal of Japan Society of Civil Engineers, Ser. A, 92-105, 2010.